The Nuclear Equation of State from Experiments and Astronomical Observations

Rohit Kumar (kumar@frib.msu.edu)

FRIB, MSU

Betty Tsang (FRIB, MSU) | William Lynch (FRIB, MSU) | C. Y. Tsang (FRIB, MSU) | C. J. Horowitz (FRIB, MSU| IU)





MICHIGAN STATE UNIVERSITY

U.S. DEPARTMENT OF ENERGY | Office of Science

Equation of State of Dense Nuclear Matter at RIBF and FRIB, 23-26th May 2023

Outline

- Constraints from nuclear experiments and astrophysical observations
- Bayesian framework
- Results on nuclear equation of state and neutron star properties
- Sensitivity analysis of constraints on the nuclear equation of state

Constraints from nuclear experiments and astrophysical observations

Nuclear experiments

Nuclear Structure/Nuclear masses/GMR /HICs

- **Dipole polarizability**

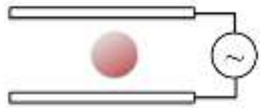

Tamii 2016

- **^{208}Pb neutron skin (PREX-II)**

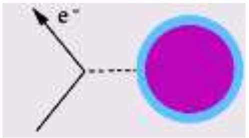

PRL 108, 112592 (2012)

- **Isobaric Analog States**
- **Nuclear masses**
- **Giant Monopole Resonance Studies**

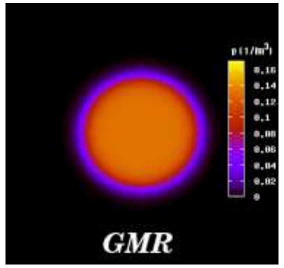

Heavy-ion collisions

Elliptical and collective Flow

Isospin diffusion

n/p spectra ratios

pion spectral ratios

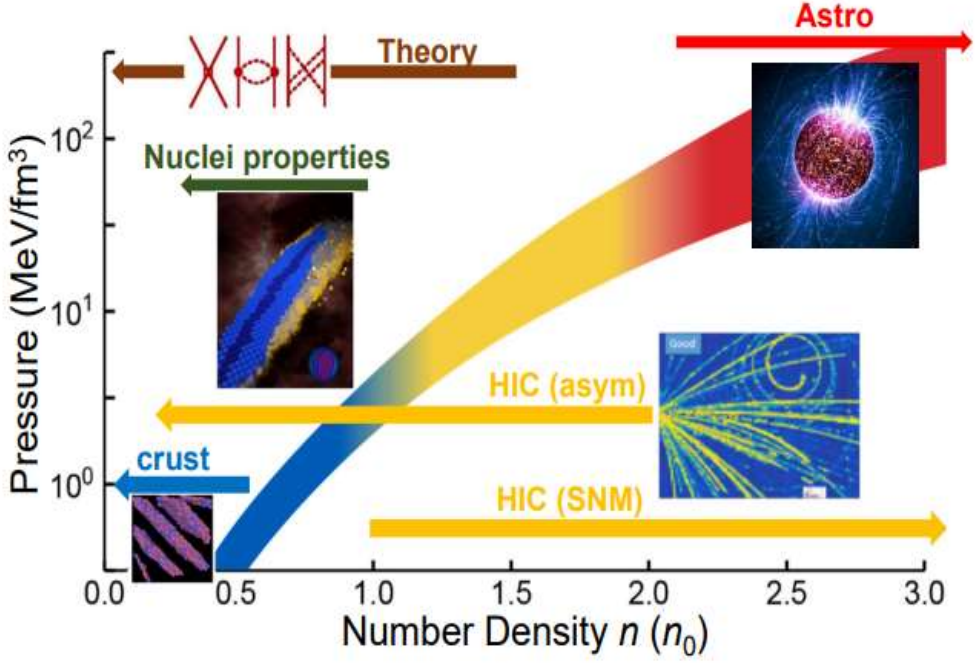

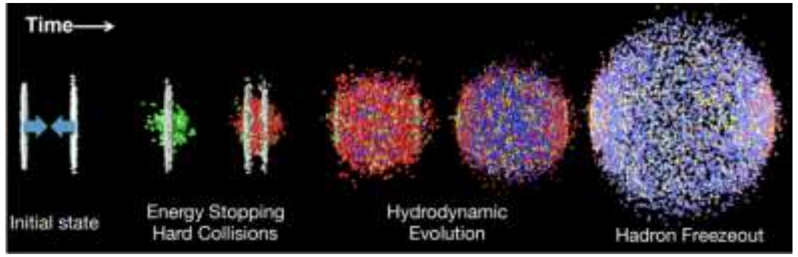

Astrophysical observations

Tidal deformability of neutron star (GW170817)

LIGO/VIRGO

Mass and Radius measurements of the neutron stars

NICER /XMM-Newton

PSR J0030+0451
PSR J0740+6620

Constraints from nuclear experiments (nuclei properties)

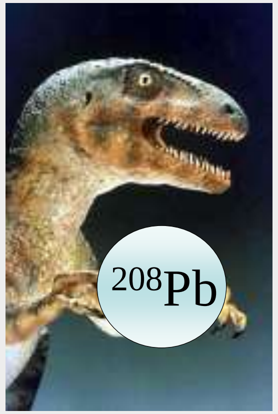

Jefferson Lab

- **^{208}Pb neutron skin (PREX-II):**
  n=0.67n_0, P_{sym}=2.38±0.75 MeVfm^{-3}
  PRL 126, 172502 (2021);PRL 126, 172503 (2021)

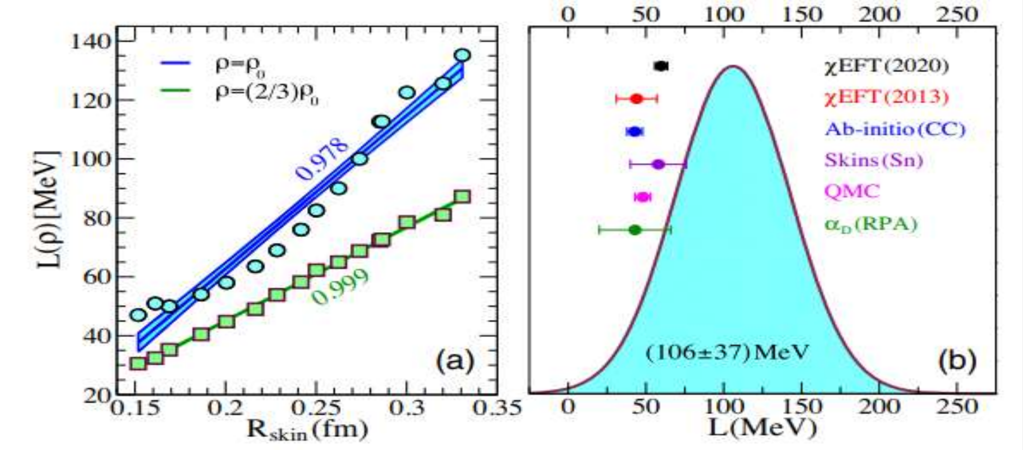

- **Isobaric Analog States (IAS):**
  n=0.66n_0; S(n) =25.5±1.1 MeV
  NPA 958, 147 (2017)
- **Mass (Skyrme):**
  n=0.63n_0; S(n)=24.7±0.8 MeV
  PRL 111, 232502 (2013); PRC 89, 011307(R) (2014)
- **Mass (DFT):**
  n=0.72n_0; S(n)=25.4±1.1 MeV
  PRC 82, 024313 (2010); PRC 85, 024304 (2012)

- **Dipole polarizability (α_D) of ^{208}Pb :**
  n=0.31n_0, S(n)=15.9±1.0 MeV
  PRC 92, 031301(R) (2015)

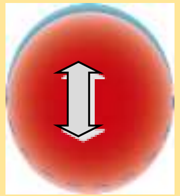

E1-field

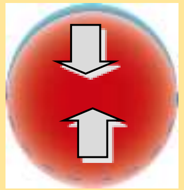

restoring force
symmetry energy

Lynch and Tsang, Phys. Lett. B 830,137098 (2022)

- **GMR**: n=n_0; K_{sat}=230±30 MeV
  PRL 82, 691 (1999); PRC 85, 035201 (2012)
  GMR strength distributions in ^{40}Ca, ^{90}Zr, ^{116}Sn, ^{144}Sm and ^{208}Pb

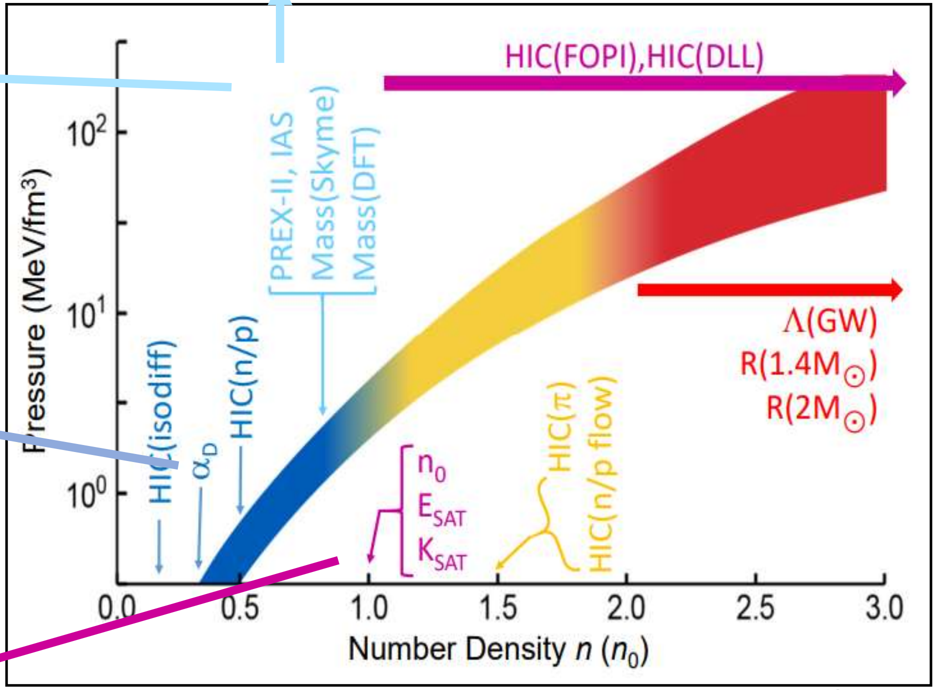

Heavy-ion collisions

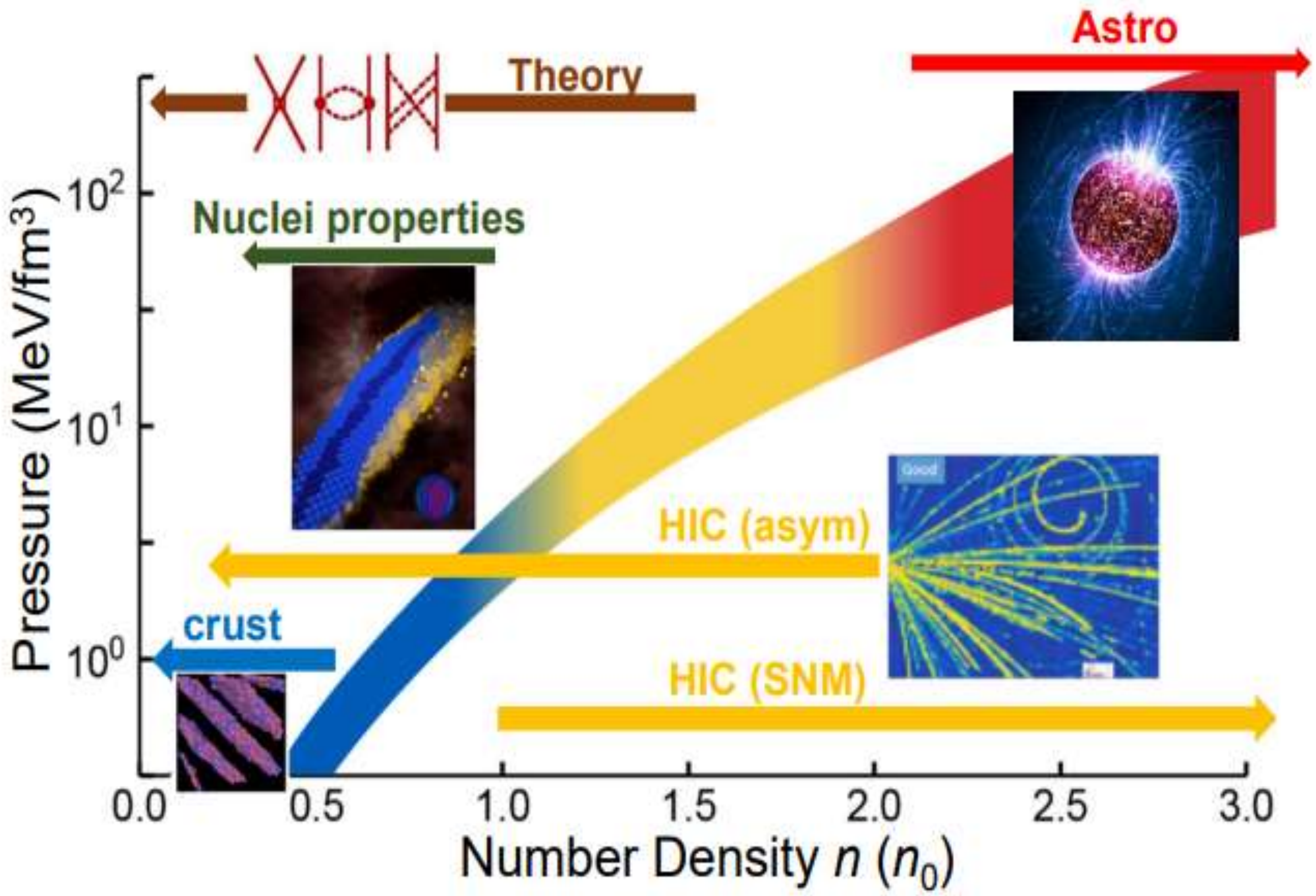

Sub-saturation densities:

- n/p & t/^{3}He
- Isospin diffusion/transport
- Neutron-proton differential flow
- Isospin scaling

Supra-saturation densities:

- Charged pion & Kaon ratios
- n/p differential transverse flow
- Nucleon elliptic flow at high transverse momentum
- n/p ratio of squeezed out nucleons perpendicular to the reaction plane

Constraints from heavy ion collisions (symmetric nuclear matter)

HIC (DLL):

- Au + Au collision data in the energy range of 0.15 to 10 GeV/nucleon
- Transverse and elliptical flow were studied
- Flow data exclude very repulsive and very soft equations of state

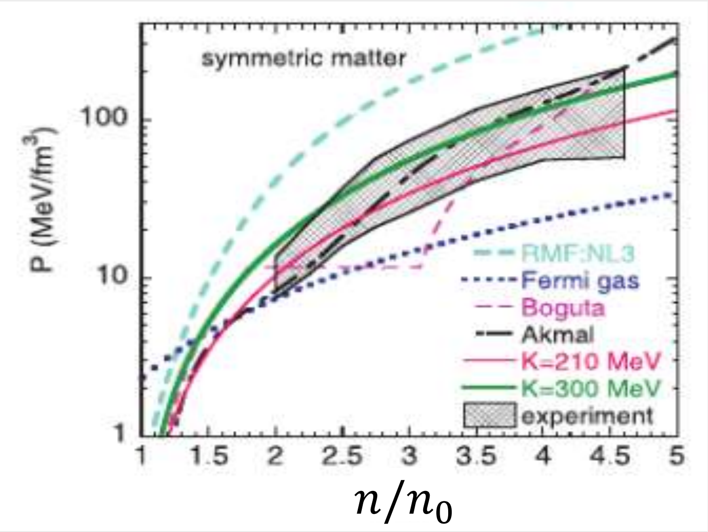

Danielewicz, Lacey, Lynch, Science 298, 1592 (2002)

HIC (DLL):
$n=2n_0$; $P_{SNM}=10.1\pm3.0$ MeVfm^{-3}
Science 298, 1592 (2002)

HIC (FOPI):
$n=2n_0$; $P_{SNM}=10.3\pm2.8$ MeVfm^{-3}
NPA 945, 112 (2016)

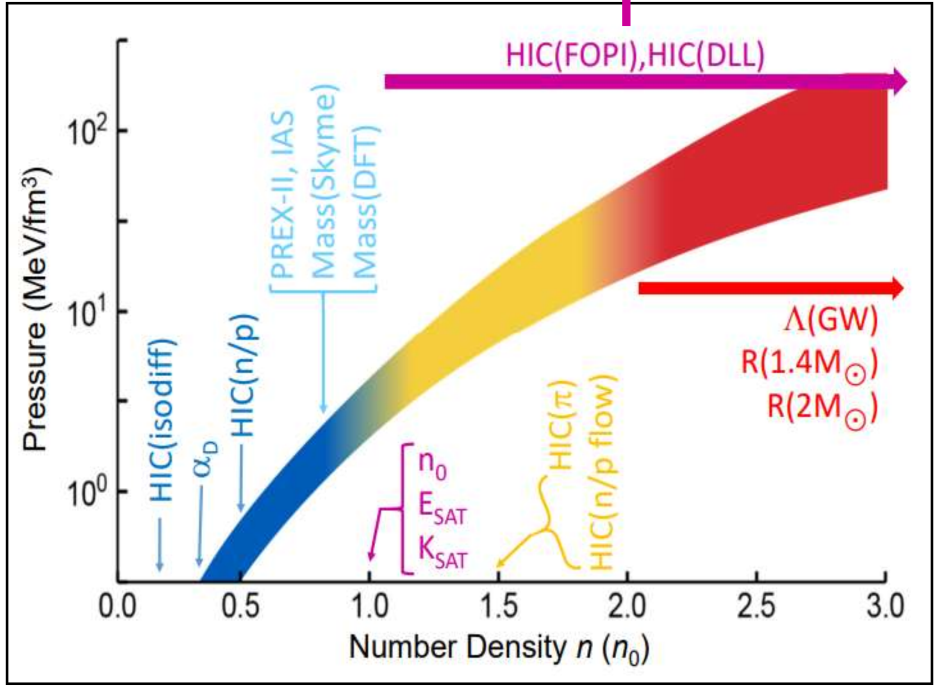

HIC (FOPI):

- FOPI experiments of Au+Au collisions at 0.4 to 1.5 GeV/nucleon
- Elliptic flow of protons and heavier isotopes

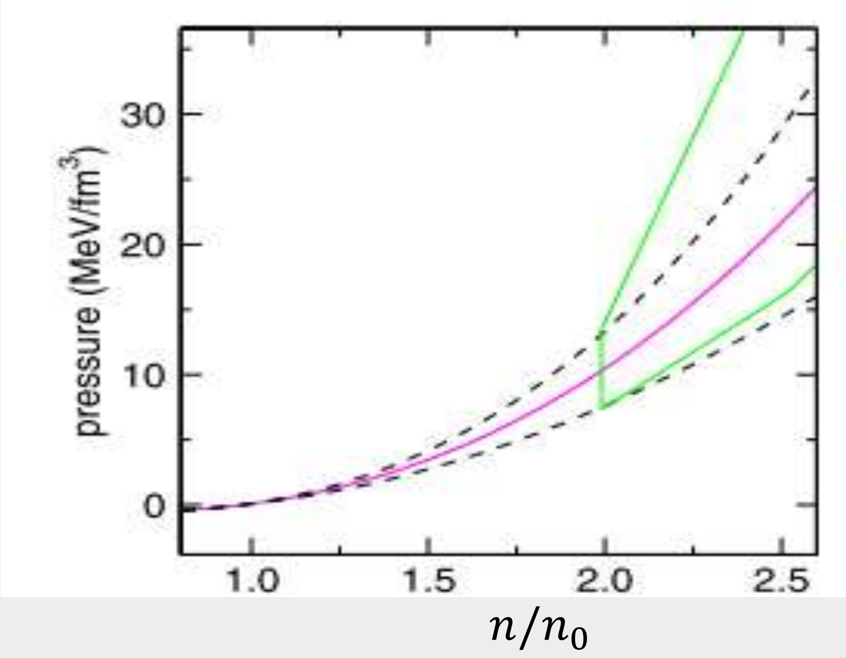

Nuclear Physics A 945, 112 (2016)

Constraints from heavy ion collisions (symmetry energy)

- **HIC Isospin diffusion:**
  $n=0.22n_0$; $S(n)=10.3\pm1.0$ MeV
  PRL 102, 122701 (2009)

- Isospin diffusion data of $^{124,112}Sn + ^{124,112}Sn$ at 50 MeV/nucleon

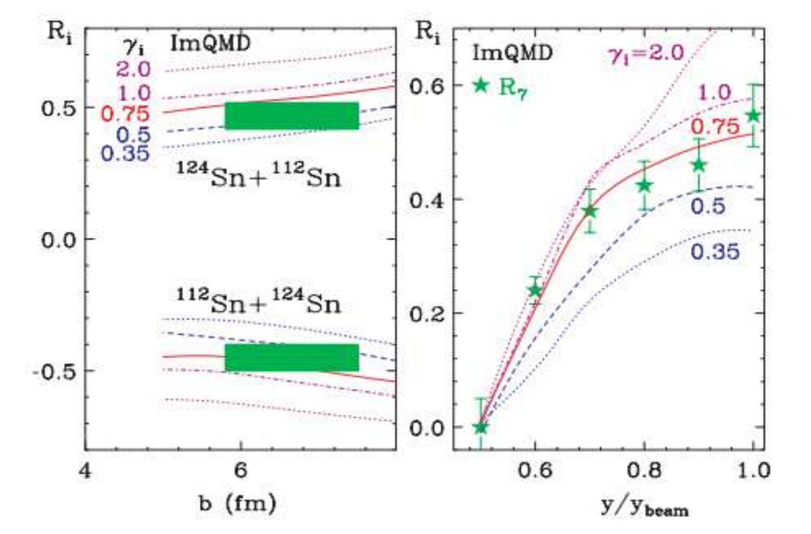

Phys. Rev. C 102, 122701 (2009)
Phys. Lett. B 830,137098 (2022)

Experimental data: NSCL, MSU

- **HIC n/p spectral ratio:**
  $n=0.43n_0$; $S(n)=16.8\pm1.2$ MeV
  PLB 799, 135045 (2019)

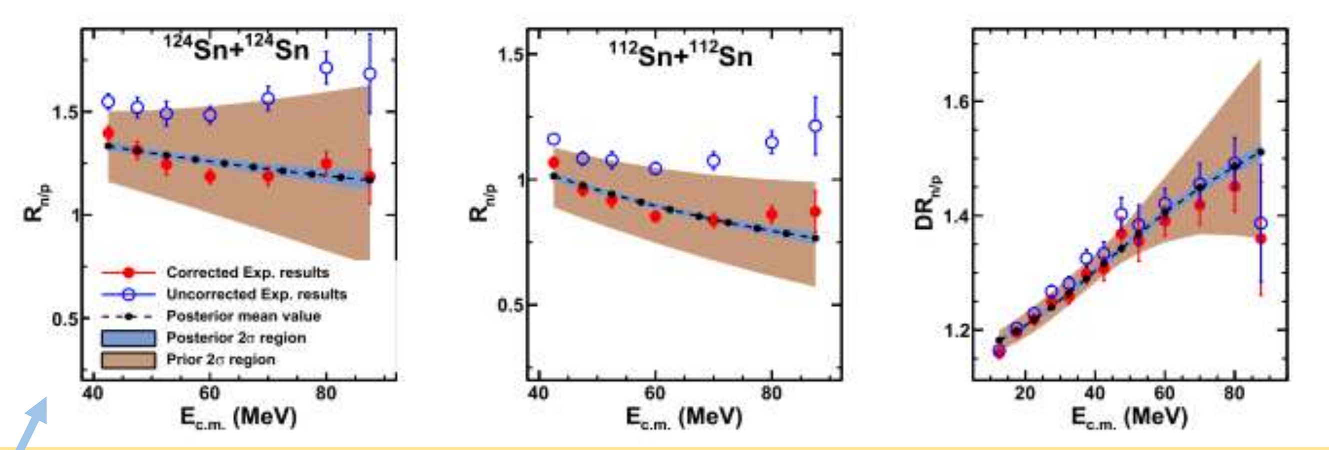

- Single ratios of neutron and proton spectra & double ratios of $^{112}Sn+^{112}Sn$ and ^{124}Sn + ^{124}Sn collisions at an incident energy of 120 MeV/nucleon

Phys. Lett. B 799, 135045 (2019)

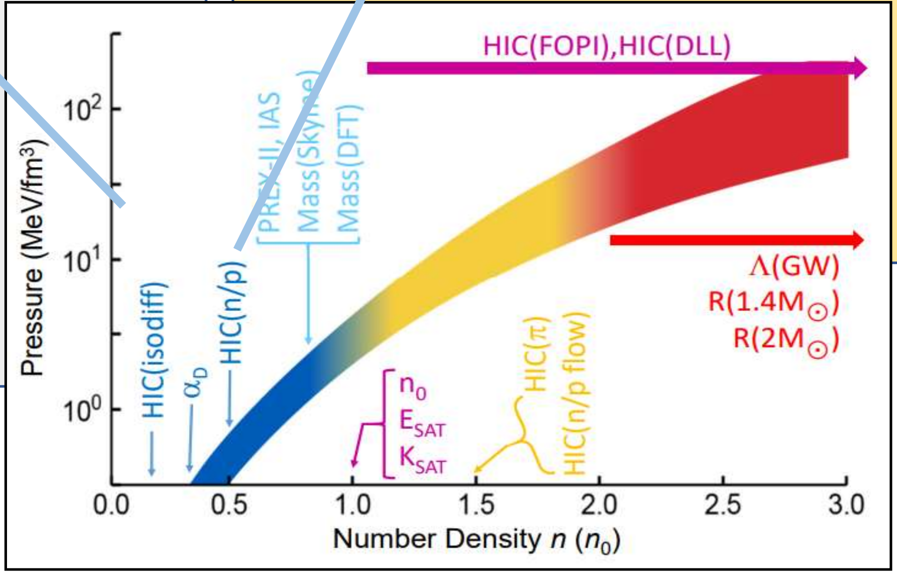

low density

Constraints from heavy ion collisions (symmetry energy)

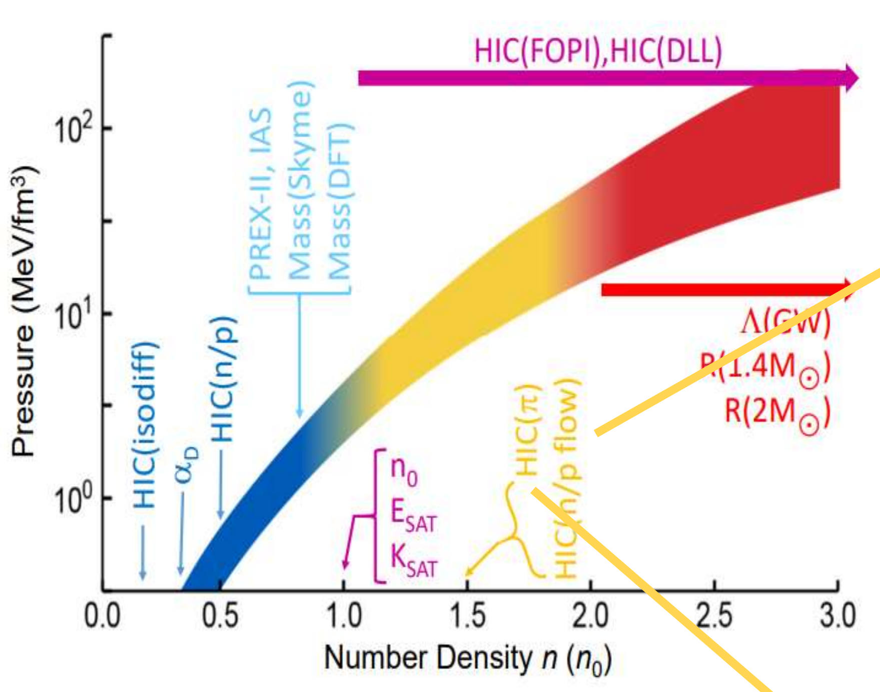

- **HIC n/p flow:**
  $n=1.50n_0$; $P_{sym}=12.1\pm8.4$ MeVfm^{-3}
  PRC 94, 034608 (2016); EPJ A 54, 40 (2018)

- Au+Au collisions at an incident energy of 400 MeV/nucleon
- FOPI-LAND neutron-to-proton and ASY-EOS neutron–to–charged-particles elliptical flow ratios data

Phys. Lett. B 697, 471 (2011)
Phys. Rev. C 94, 034608 (2016)
Eur. Phys. J. A 54, 40 (2018)

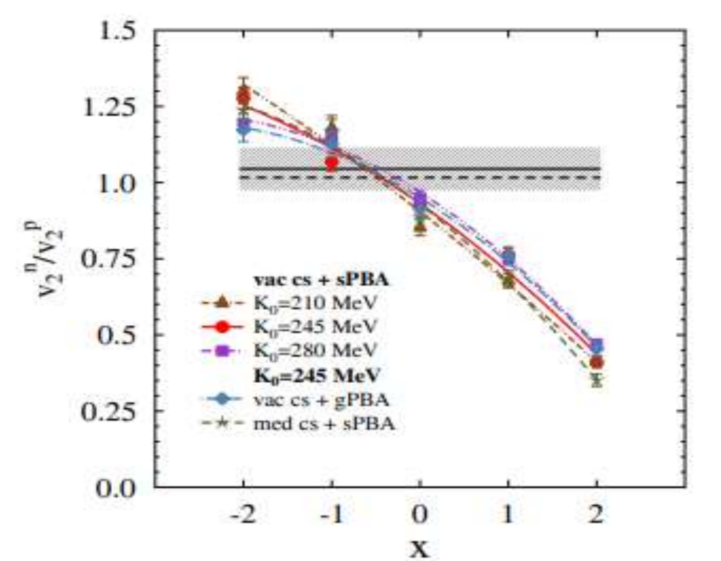

- **HIC pion spectral ratios:**
  $n=1.45n_0$; $S(n)=52\pm13$ MeV,
  $P_{sym}=10.9\pm8.7$ MeVfm^{-3}
  PRL **126**, 162701 (2021)

- ^{132}Sn +^{124}Sn and ^{108}Sn +^{112}Sn incident energy of 270 MeV/nucleon
- Observables: Charged pion transverse momentum spectra

PRL **126**, 162701 (2021)

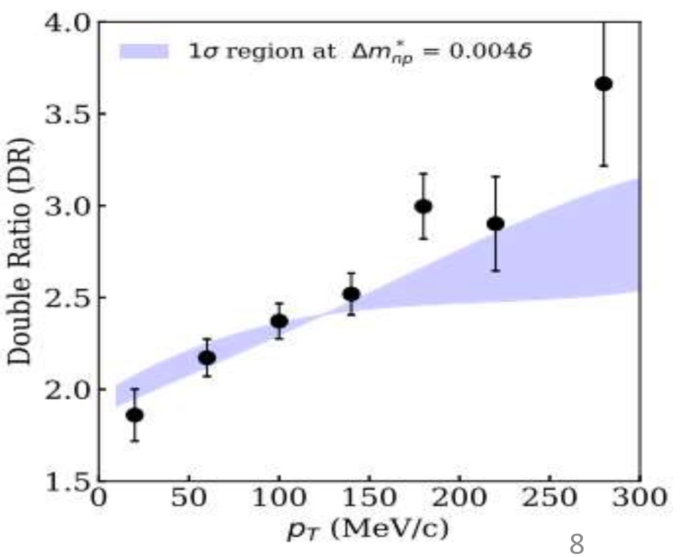

high densities

See also talks by C. Y. Tsang and W. Lynch

SPiRIT TPC experiments at RIKEN

Constraints from astrophysics observations

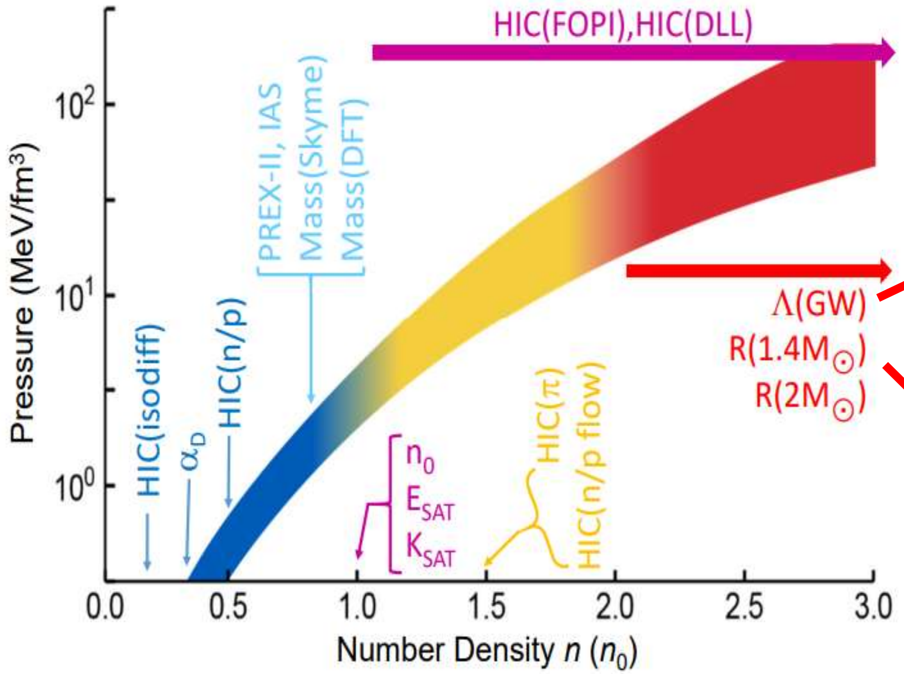

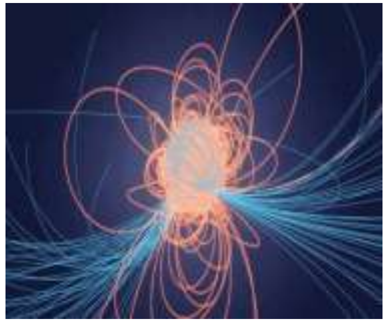

Gravitational tidal field distorts shapes of neutron stars just before they merge

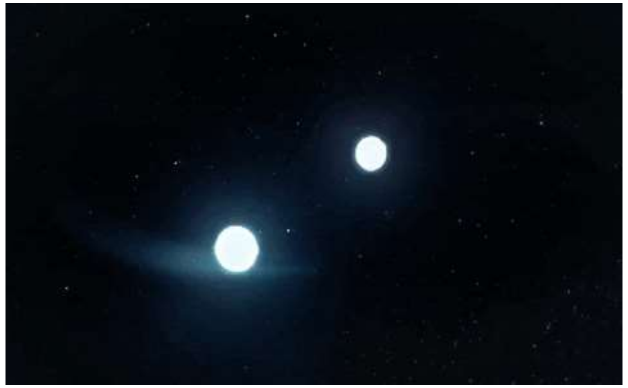

- **Tidal deformability:**

$$\Lambda\left(\mathrm{M} = 1.4\ \mathrm{M}_{\odot}\right) = 190^{+390}_{-120}$$

PRL 119, 161101 (2017); PRL 121, 161101 (2018)

- **PSR J0030+0451**:

$$M = 1.34^{+0.15}_{-0.16} M_{\odot};\ R = 12.71^{+1.14}_{-1.19}\ km$$

Riley et al APL 887, L21 (2019)

$$M = 1.44^{+0.15}_{-0.14} M_{\odot};\ R = 13.02^{+1.24}_{-1.06}\ km$$

Miller et al APL 887, L24 (2019)

- **PSR J0740+6620:**

$$M = 2.07^{+0.07}_{-0.07} M_{\odot};\ R = 12.39^{+1.30}_{-0.98}\ km$$

Riley et al APL 918, L27 (2021)

$$M = 2.08^{+0.07}_{-0.07} M_{\odot};\ \ R = 13.7^{+2.6}_{-1.5}\ km$$

Miller et al APL 918, L28 (2021)

Two independent analysis (with different emission geometry assumptions)

Pulse profile modeling of hot spots on the rapidly rotating neutron stars

Bayesian analysis

Posterior — Prior — Likelihood

$$P(\mathrm{EoS}|\mathrm{Constraints}) \propto P(\mathrm{EoS}) \prod_i \mathcal{L}(i^{\mathrm{th}}\ \mathrm{Constraint})$$

MetaModeling EoS: No inbuilt correlations among parameters, wide enough to include all data points

15 total constraints from nuclear experiments and astrophysical observations

Priors

Nuclear experiments
Astrophysical observations

Predictions for
Nuclear EOS

Predictions for Neutron star properties

Priors

Uniform prior distribution P(M) in the ranges of

Parameters	Priors
K_{SAT} (MeV)	[0, 648]
Q_{SAT} (MeV)	[-1100, 2100]
S_0 (MeV)	[24.7, 40.3]
L (MeV)	[-11.4, 149.4]
K_{sym} (MeV)	[-328.5, 237.9]
Q_{sym} (MeV)	[-489, 1223]
Z_{sym} (MeV)	[-10110, 2130]
Z_{SAT} (MeV)	

Any reliable nuclear EoS should give a stable neutron star, otherwise is rule out

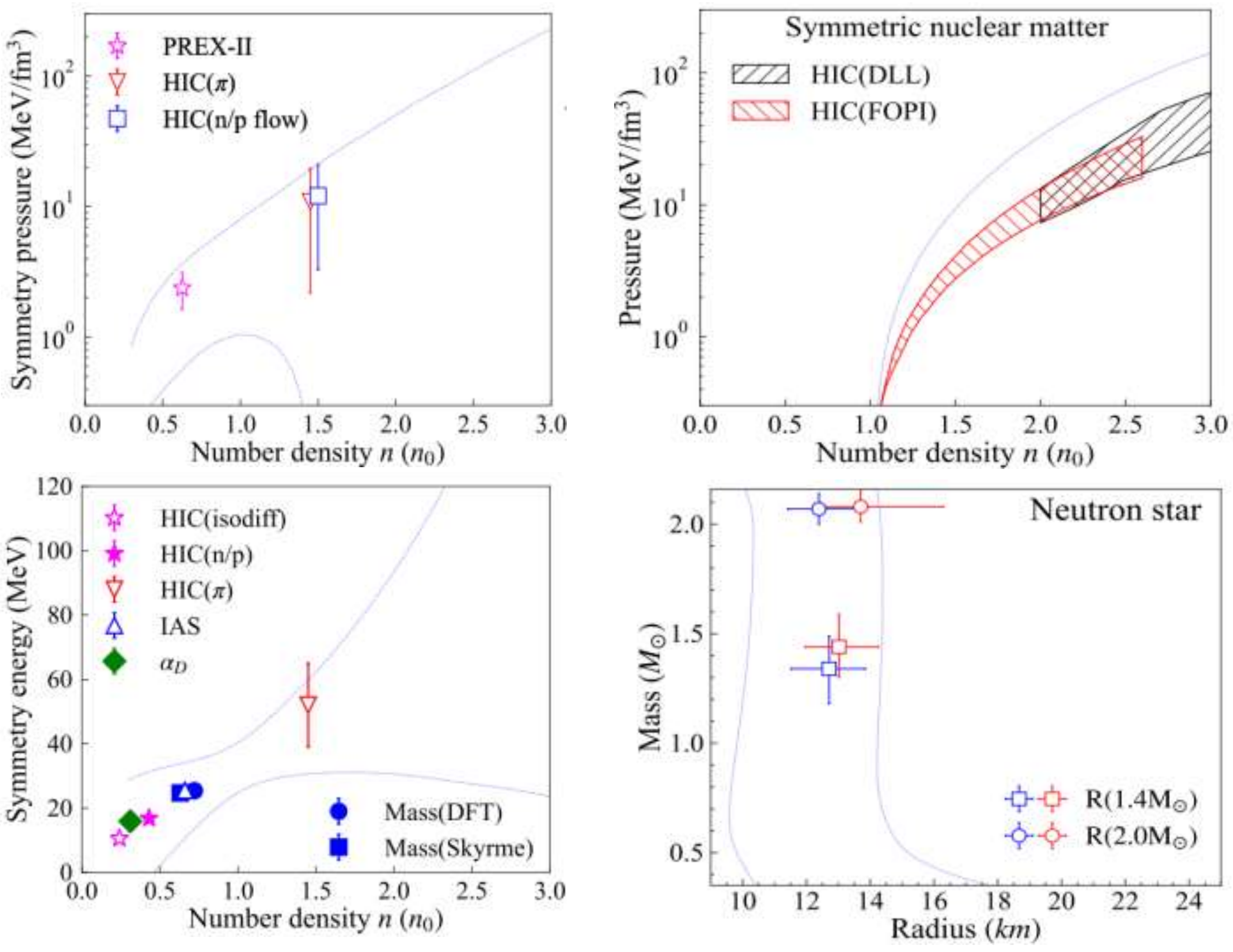

Predictions for Nuclear EOS

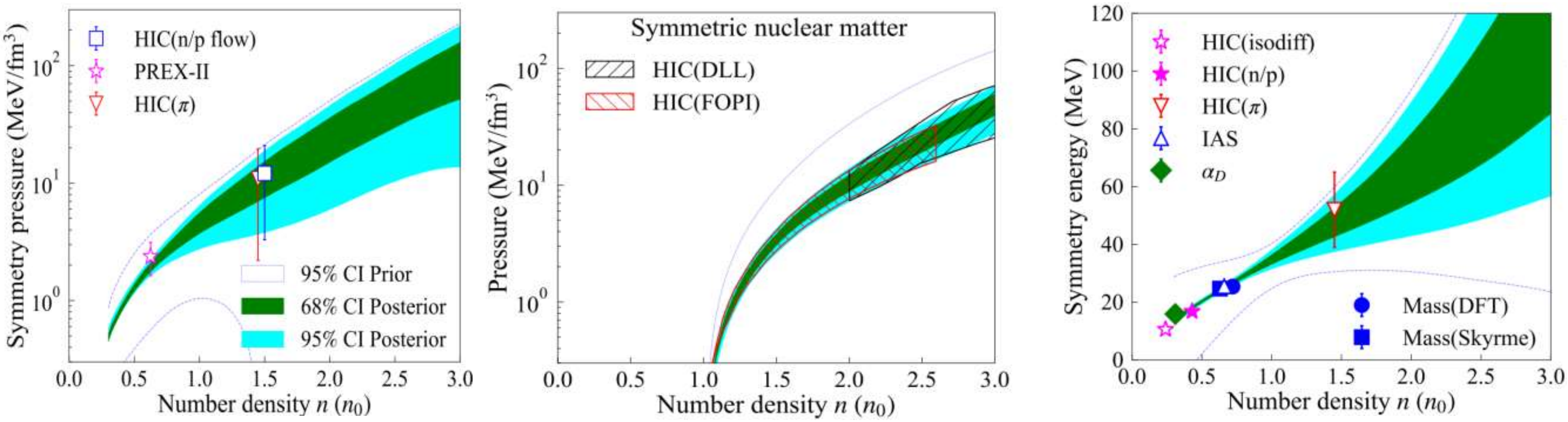

- Uncertainty in predictions increases with increase in the density
- Combining nuclear data with astrophysical observations better constraints the EoS
- Need to reduce the error bars for HIC data in the density range of 1-2n_0
- More data points needed in the density range of 1-2n_0

Benchmarking equation of state for nuclear theory

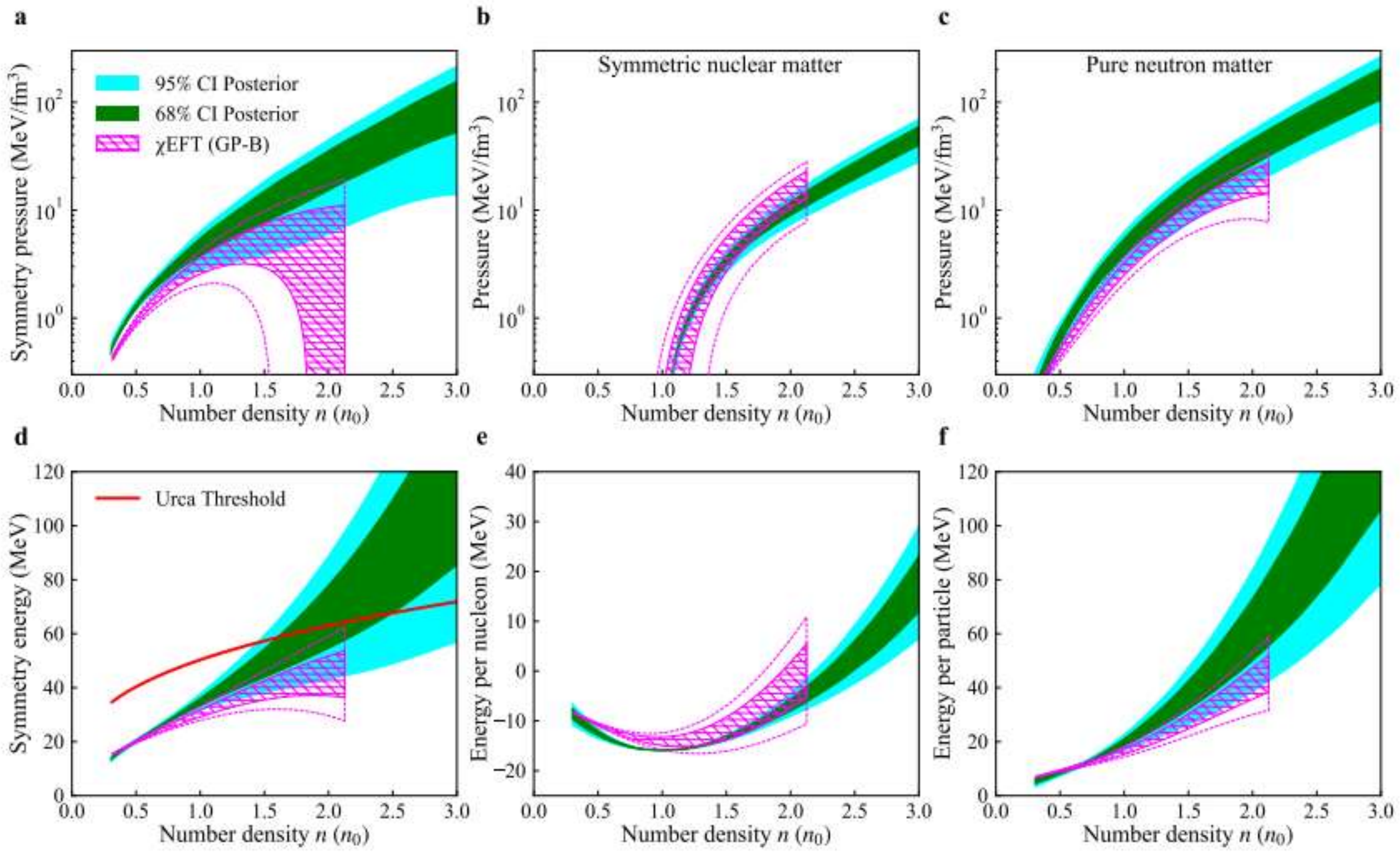

Results only directed by nuclear experiments
And astrophysical observations

Comparison with Chiral Effective Field theory results

Drischler et al., PRL 125, 202702 (2020)
PRC 102, 054315 (2020)
PRL 122, 042501 (2019)

Predictions for Neutron stars

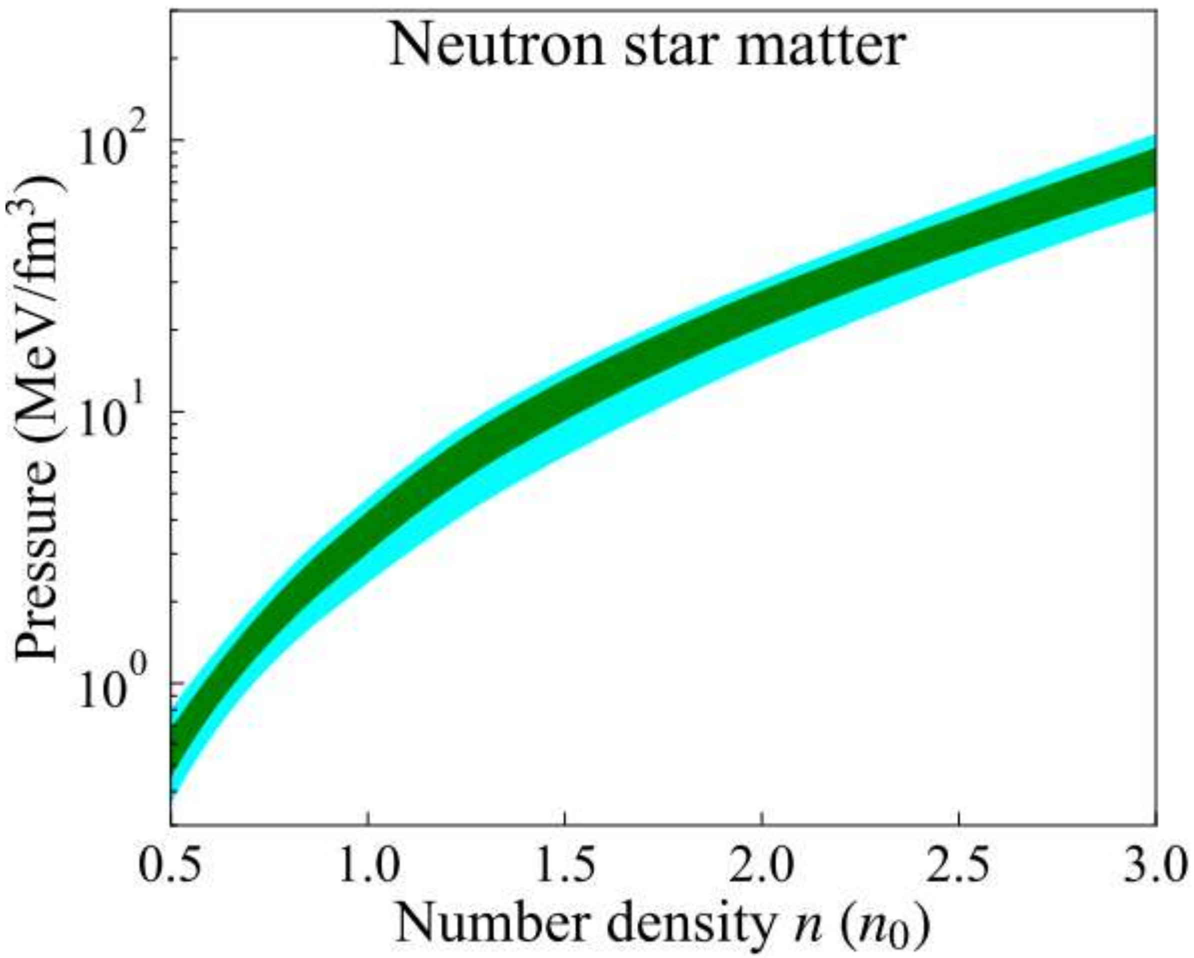

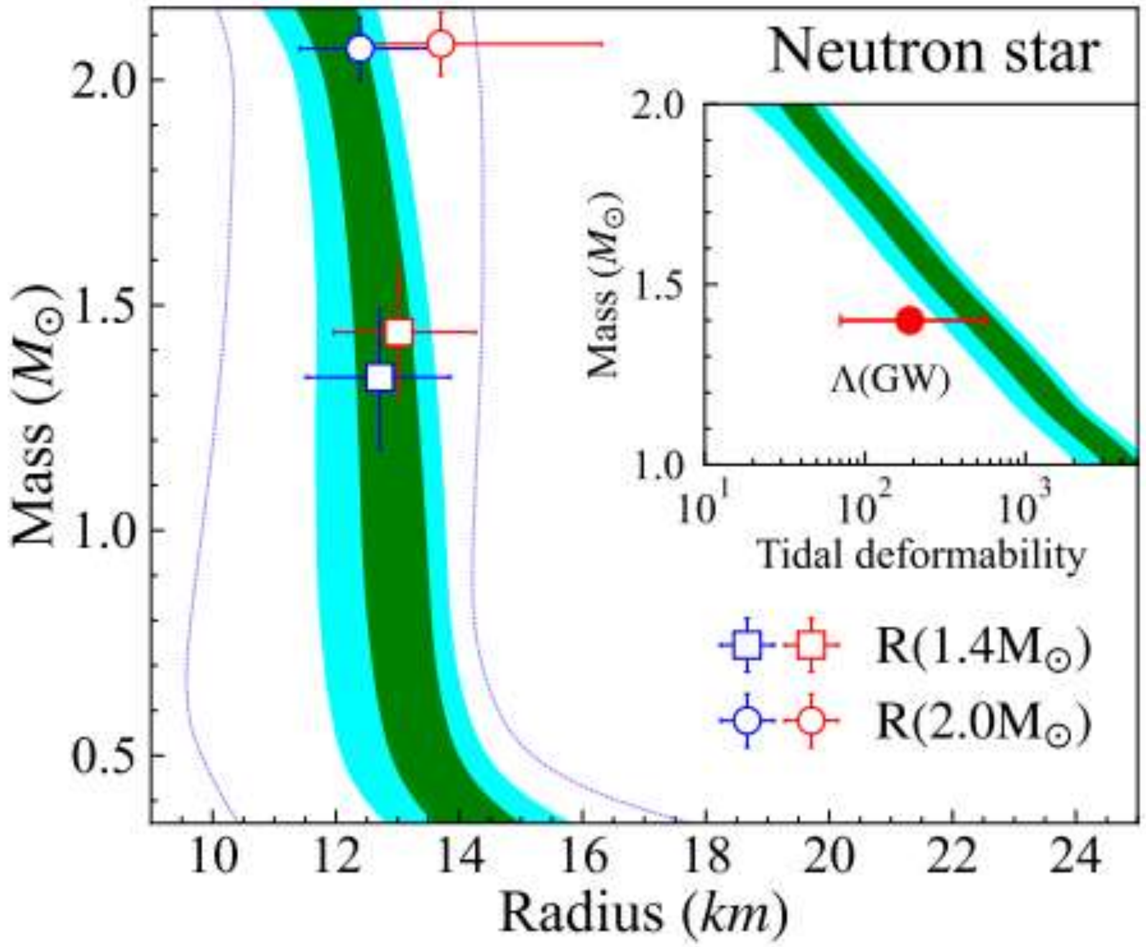

Neutron star equation of state

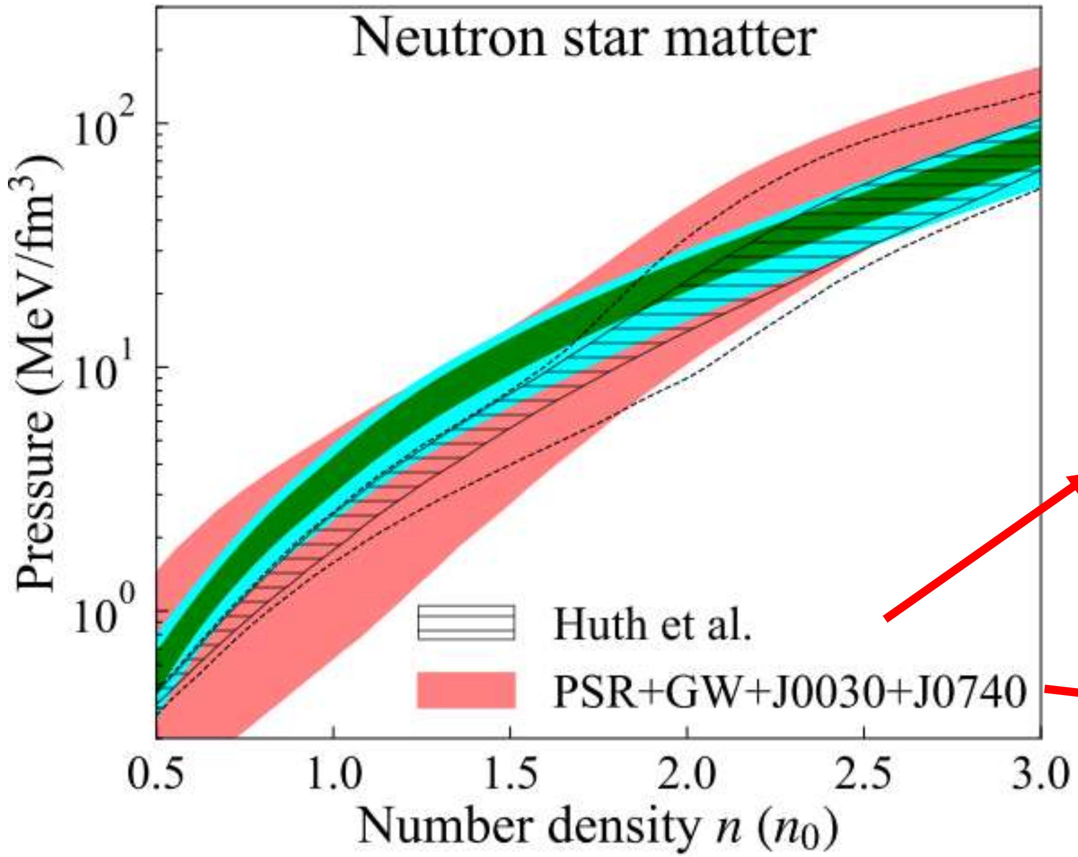

Huth, Pang et al., Nature 606, 279 (2022)

Chiral Effective Field theory (upto 1.5n_0)

Heavy-ion collision constraints

Astrophysical observations

Legred et al., Phys. Rev. D 104, 063003 (2021)

Non-parametric EOS

Astrophysical observations

- Combining nuclear experiments with astrophysical observations also helps to reduce the Uncertainties in the predictions of neutron star EoS and their properties

Direct URCA process

The symmetry energy is very important to understanding the composition and dynamics of matter within neutron stars because it contributes to the chemical potentials of the particles that compose the stellar matter.

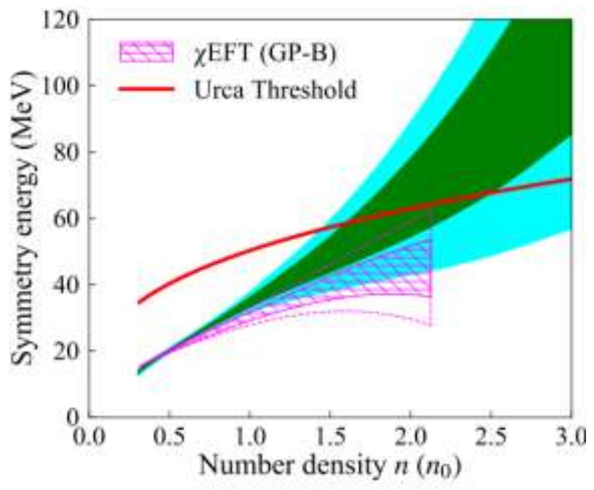

In β-equilibrium the chemical potentials of neutron μ_n, proton μ_p and electron μ_e satisfy $\mu_e = \mu_n - \mu_p$ and the proton fraction y_p satisfies,

$$[4S(n)(1-2y_p)]^3 + \left\{[4S(n)(1-2y_p)]^2 - m_\mu^2\right\}^{3/2} = 3\pi^2 n y_p$$

The threshold density for Urca, n_{Urca}, is the lowest density where

$$k_F^p + k_F^e > k_F^n$$

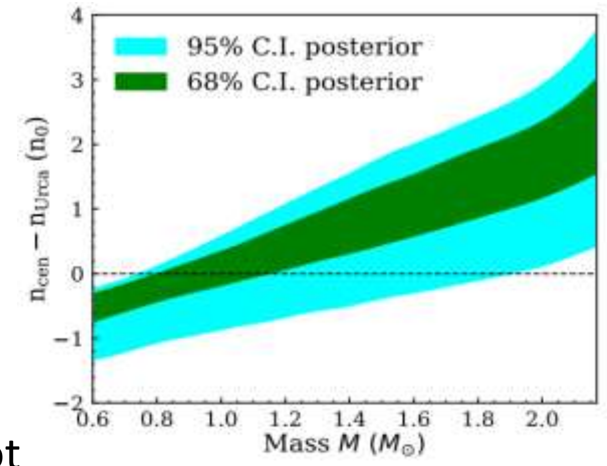

Note, neutron star cooling depends on possible super fluid pairing gaps in addition to y_p but not considered in the present work

Sensitivity analysis of different constraints

Without PREX-II constraint

All 15 constraints

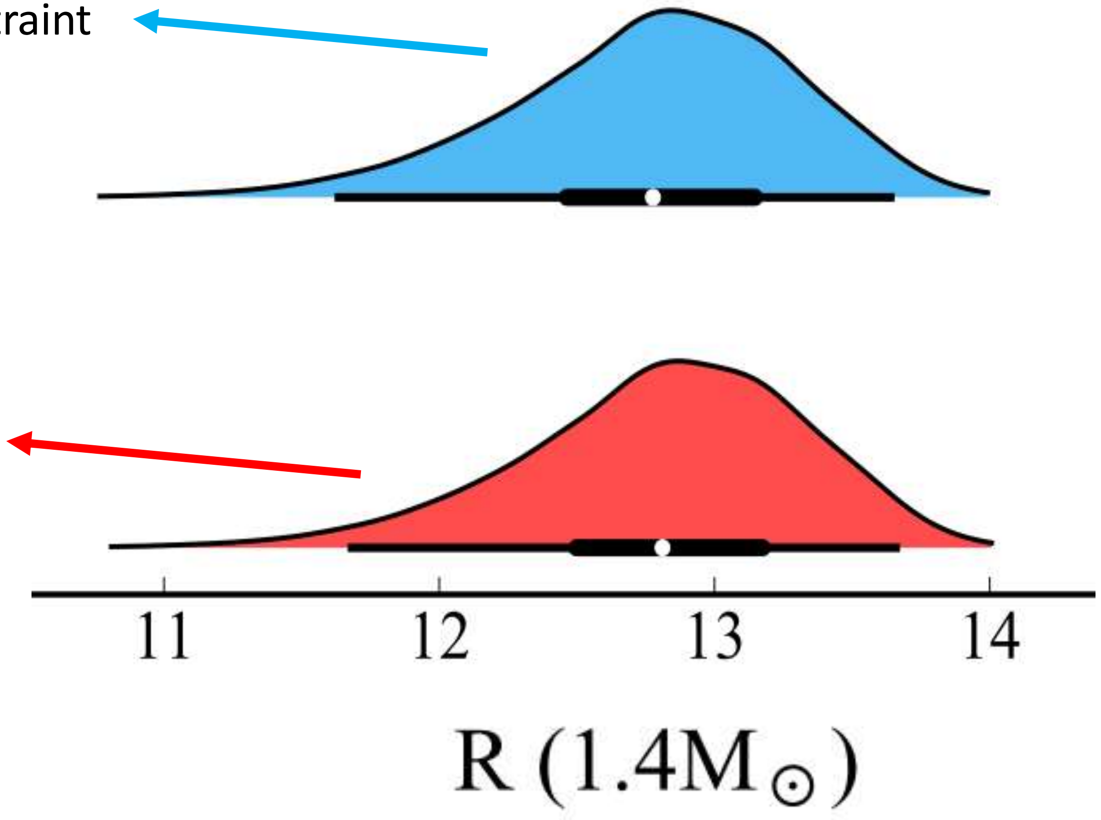

Remove PREX-II constraint

No significant effect on neutron star radius

Role of different constraints

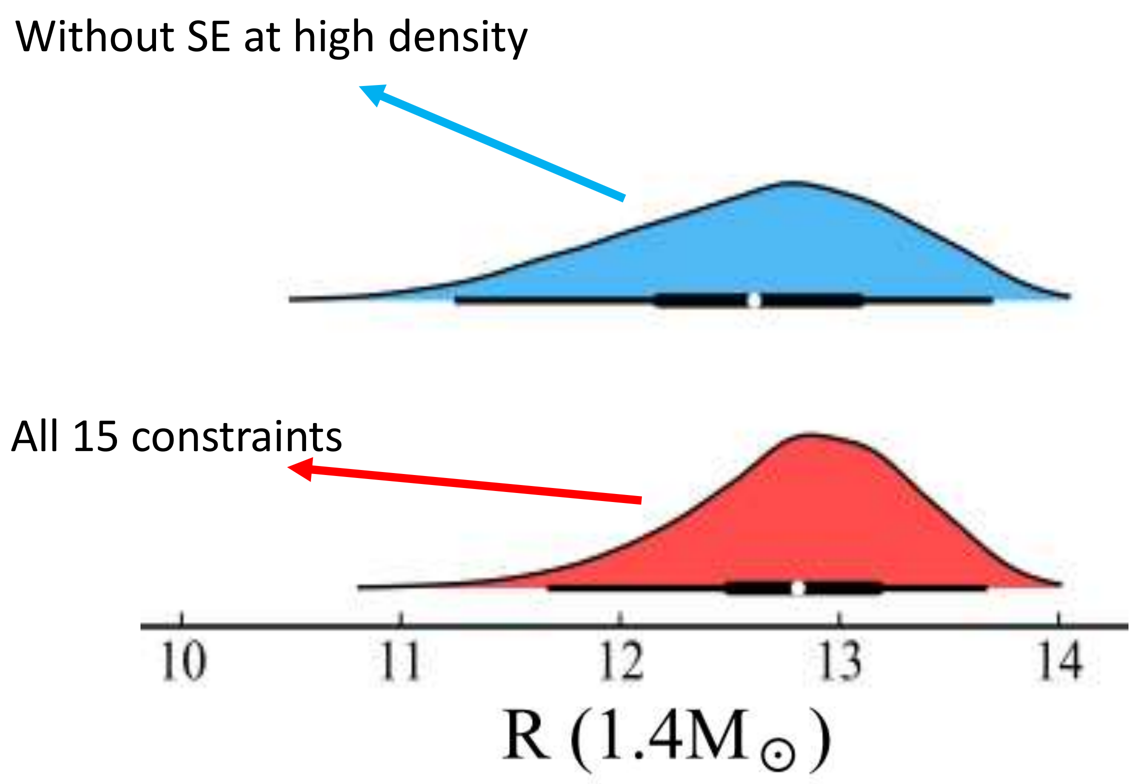

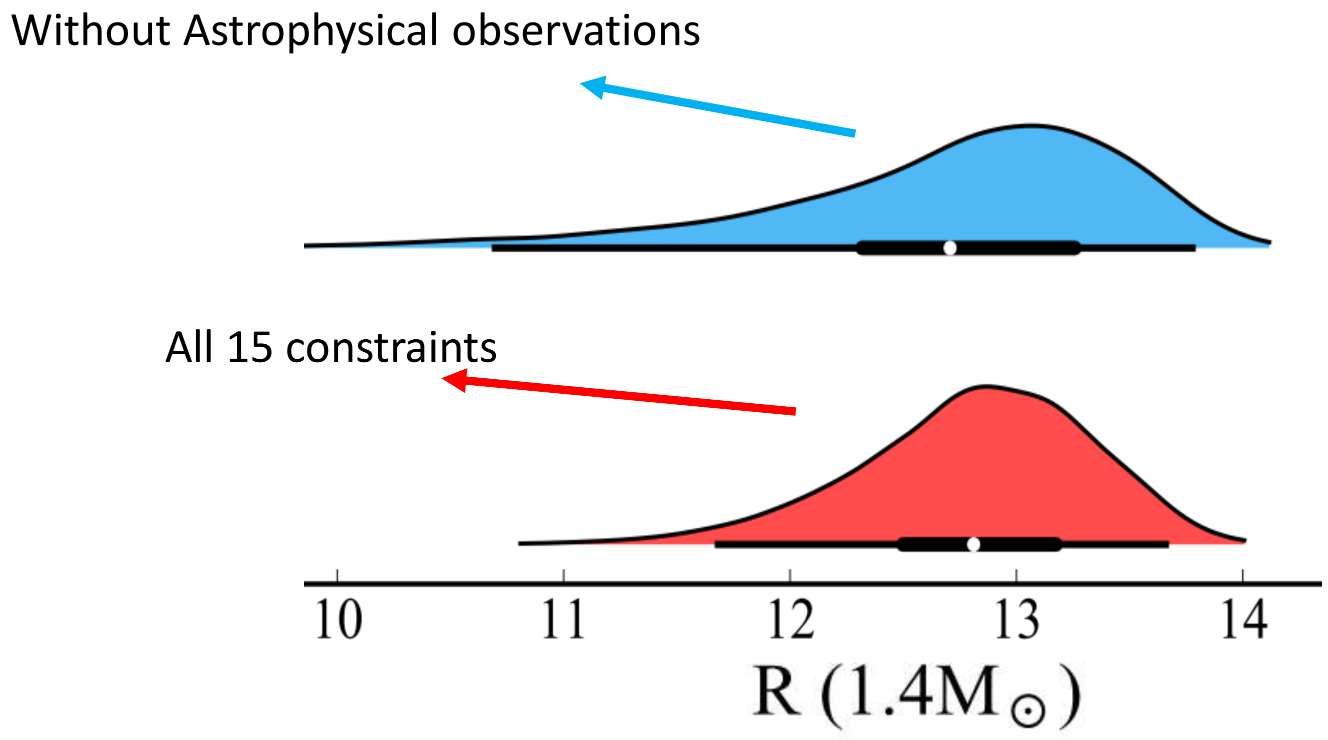

Further improvements in the future

50% Reduced errors
HIC + Astro observation

50% Reduced errors
Astrophysical observations

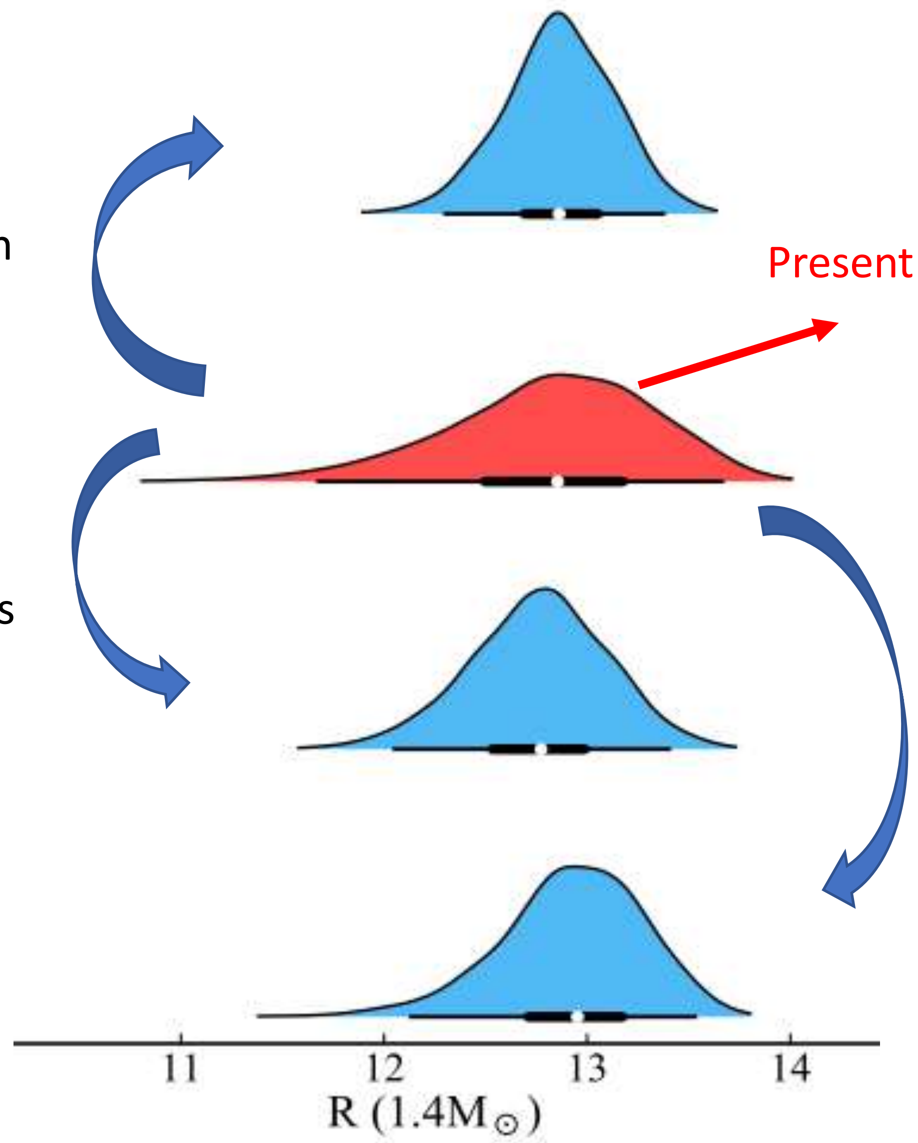

Present: all 15 constraints

50% Reduced errors
HIC results

Strongest constraining power

HIC constraints
+
astrophysical observations

Need of improvements on HIC results and astrophysical observations

Summary

- We have constrained the equation of state using the existing constraints from nuclear structure, masses, monopole resonance studies, heavy-ion collision studies and astrophysics observations.
- One can use these results as benchmarking equation of state for future developments of theories
- Adding heavy-ion collisions constraints at higher densities helps to tighten the predictions on equation of state
- Constraints from symmetric nuclear matter (FAIR, RHIC)
- Better constraints on symmetry energy at supra-saturation densities (ASY-EOS, RIBF, FRIB & FRIB400)
- Next measurements from NICER, LIGO/VIRGO, eXTP and STROBE-X

➢You for your time and attention

This work is supported in part by the National Science Foundation (NSF) under Grant No. PHY-2209145 and the US Department of Energy Office of Science Office of Nuclear Physics grant no. DE-FG02-87ER40365